Acta Biochimica Polonica

Vol. 44 No. 3/1997

453–466

QUARTERLY

Minireview

Elucidation of neurophysin/bioligand interactions from molecular modeling*

Rajmund Kaźmierkiewicz, Cezary Czaplewski and Jerzy Ciarkowski✉

Faculty of Chemistry, University of Gdańsk, J. Sobieskiego 18, 80-952 Gdańsk, Poland

Key words: protein/ligand interactions, molecular dynamics, AMBER 4.1, allosteric communication

This is a review of our recent modeling work aimed at: (i) development and assessment of techniques for reliable refinement of low-resolution protein structures and (ii) using these techniques, at solving specific problems pertinent to neurophysin-bioligand interactions. Neurophysins I and II (NPI and NPII) serve in the neurosecretory granules of the posterior pituitary as carrier proteins for the neurophyseal hormones oxytocin (OT) and vasopressin (VP), respectively, until the latter are released into blood. NPs are homologous two-domain, sulphur rich small proteins (93–95 residues, 7 disulphide bridges per monomer), capable of being aggregated. The C_2 symmetrical NPI_2 and $NPII_2$ homodimers, and the $(NPI/OT)_2$ and $(NPII/VP)_2$ heterotetramers, all believed to be the smallest functional units, were modeled using low-resolution structure information, i.e. the C^{α}-carbon coordinates of the homologous NPII/dipeptide complex as a template. The all-atom representations of the models were obtained using the SYBYL suite of programs (by Tripos, Inc.). Subsequently, they were relaxed, using a constrained simulated annealing (CSA) protocol, and submitted to about 100 ps molecular dynamics (MD) in water, using the AMBER 4.1 force field. The $(NPI/OT)_2$ and $(NPII/VP)_2$ structures, averaged after the last 20 ps of MD, were remarkably similar to those recently reported either for NPII/dipeptide or NPII/oxytocin complex in the solid state (Chen *et al.*, 1991, *Proc. Natl. Acad. Sci., U.S.A.* 88, 4240–4244; Rose *et al.*, 1996, *Nature Struct. Biol.* 3, 163–169). The results indicate that the 3_{10} helices (terminating the amino domains) and the carboxyl domains are more mobile than the remainder of the NP monomers. The hormones become anchored by residues 1–3 and 6 to the host, leaving residues 4–5 and 7–9 exposed on the surface and free to move. A cluster of attractive interactions, extending from the ligand binding site, Tyr-24-Ile-26 of unit 1(2), to the inter-monomer interface Val-36 of unit 1(2), Cys-79 and Ile-72 of unit 2(1), is clearly seen. We suggest that both these interactions as well as the increased mobility of the 3_{10} helix and the carboxyl domain may contribute to the allosteric communication between the ligand and the unit1-unit2 interface.

*The work was supported by the State Committee for Scientific Research (KBN), grant No. 3 T09A 027 11; by the Interdisciplinary Center for Mathematical and Computational Modelling (ICM) at the University of Warsaw (use of CRAY Y-MP/EL-98); and by the Informatics Center for Metropolitan Academic Network (CI TASK), Gdańsk area (use of SGI Power Challenge 8xR10000 or an IBM SP2 15xPOWER2 supercomputers).

Abbreviations: NPI, neurophysin I; NPII, neurophysin II; OT, oxytocin; VP, vasopressin; CSA, constrained simulated annealing; MD, molecular dynamics; r.m.s., root-mean-square deviation.

✉To whom correspondence should be addressed; phone/fax: (+48 58)+41-03-57; e-mail: jurek@sun1.chem.univ.gda.pl.

The nonapeptide hormones oxytocin (CY-IQNCPLG-NH_2, OT) and vasopressin (CY-FQNCPRG-NH_2, VP), while becoming mature, are transported to the posterior pituitary as associates (1:1) with neurophysin I (NPI) and II (NPII), respectively. The maturation of either hormone consists in its splitting away from its respective NP counterpart, with which it originates together as one precursor [1, 2]. The NP/hormone associates are packaged at relatively high concentrations (> 0.1 M) [3] in the neuroscretory granules wherein they travel until the hormones are dissociated upon secretion into the blood. The two NPs show similar affinities to either hormone, as well as to a number of small N-terminal peptide analogues [4–6]. The interactions between the NP and the hormone segments within the precursors seem to be similar to those in the complexes and essential for correct folding of the precursors and pairing of the disulphides [7–11]. Both NPs are small disulphide-rich proteins of 93–95 amino-acid residues forming two highly homologous domains per monomer. These domains are supported by 7 disulphide bridges: 3 bridges per domain plus an inter-domain one.

Two solid-state structures of NPs are currently available: the first one for the NPII/dipeptide complex [12] and the other, recently released, for the NPII/OT (cross) complex [13]. Both three dimensional structures, while confirming extensive structural homologies and virtually identical binding modes for OT and the dipeptide analogue, provide also details on conformations of the ligands, on locations of the binding sites, and on the modes of interaction between the NPs and the ligands (Fig. 1).

Our recent interest has been the *de novo* modeling of protein-ligand interactions using sequence homology and/or low-resolution structural information as starting data. With this aim, we have recently simulated the NPII/dipeptide complex [14], using merely the C^{α}-trace as a starting frame, which at the same time was the only available data, those deposited by Chen *et al.* [12] in the Brookhaven Protein Data Bank [15] as file 1BN2. Our simulation led to a complex that overlapped well with the reference C^{α}-trace and also perfectly reproduced all key interactions between the protein and the ligand. Subsequently, we have simulated the NPI/OT and NPII/VP complexes and received also very satisfactory results [16, 17]. In this work we review these efforts and present our new CSA protocol of general use in molecular modeling.

METHODS

The initial all-atom (NP/ligand)$_2$ heterotetramers were generated from the respective C^{α}-trace (units 1 and 2 in file 1BN2, Brookhaven PDB [15]) using the Biopolymer module of the SYBYL suite of programs [18], as described in detail in the original papers [14, 16, 17]. The neurophysin-bound structure of a ligand was based on an NMR-derived conformation of oxytocin bound to neurophysin I [19], including subsequent corrections suggested by Breslow *et al.* [20]. The initial all-atom homodimers NPI_2 and $NPII_2$ were generated by mechanical removal of ligands from the respective heterotetramers. All high-power computing, consisting of molecular mechanics and/or dynamics (MD) calculations, was executed using AMBER v. 4.1 suite of programs [21]. MD simulations were carried out in water with periodic boundary conditions imposed. A typical computational protocol is given in Table 1. More details concerning computations are given in the original papers [14, 16, 17]. The molecular images for presentation were prepared using either RasMol [22] or MOLSCRIPT [23] programs.

RESULTS AND DISCUSSION

The analyses of time evolution of energy (not shown) reveal that both the homodimers and the heterotetramers, after intensive initial energy changes need not more than 20 ps to achieve reasonably stabilized fluctuations in time [14, 16, 17], when refined in accordance with the protocol in Table 1. A typical evolution of geometry during MD is given in Figs. 2 and 3 for the (NPII/VP)$_2$ heterotetramer and the $NPII_2$ homodimer,

A

NPII MS EL Q_{10} 20 30 40
NPI AVLDLDVRTCLPCGPGGKGRCFGPSICCGDELGCFVGT**AEALRCQEENY**

50 60 70 80 90
NPI *LPSPCQSGQ*KPCGSG- - GRCAAAGICCSPDGCHED*PACD.PEAAFSQ*
NPII NDES VTE E R.EGVGFPRRV

B

Figure 1A. The sequences of bovine neurophysins I and II (NPI and NPII).

The β-strands are underlined, the 3_{10} helix is printed in bold and the inter-domain connection in italics. The C-terminal fragment, not included in the solid state structure [12], is separated by a dot. The homologous fragments in the amino and carboxyl domains are aligned vertically one under the other.

Figure 1B. The structure of a NPII/dipeptide heterodimer [12] built up of the C^{α}-carbon coordinates (file 1BN2 from the Brookhaven Protein Data Bank [15]).

The NPII molecule is made up of two highly homologous domains, composed of similar four-stranded antiparallel β-sheets. In the amino domain the β-sheet is immediately followed by a 3-turn 3_{10} helix, having no match in the carboxyl domain. The two domains are connected by a relatively loose backbone fragment, supported by an *inter*-domain disulphide bridge C10–C54. The remaining 6 disulphide bridges crosslink the *intra*-domain residues: the bridges 13–27, 21–44 and 28–34 within the amino domain and the bridges 61–73, 67–85 and 74–79 within the carboxyl domain. The dipeptide ligand, represented by a stick model, is seen in the binding loop (ENYLPSPC, 47–54) composed of the end of the 3_{10} helix (AEALRCQEENY, 39–49) and the beginning of the inter-domain connection (LPSPCQSGQ, 50–58). The figure was generated using MOLSCRIPT [23].

respectively. The $(NPI/OT)_2$ and NPI_2 complexes behaved in a very similar way [16]. The intensive energy changes at the start of each MD simulation were not correlated with changes in geometry. Thus, the initial energy changes could likely be due to an accommodation to and/or penetration of water molecules through the protein surface into the protein body.

From Figs. 2 and 3 it is seen that, if the N-termini of the proteins and the VP carboxyl tails are disregarded, the root-mean-square (r.m.s.) deviations measured relative to the starting structures do not exceed about 2 Å.

Detailed inspection of the final averaged structures, (Figs. 4 and 5) suggests the existence of two sets of symmetry-related inter-monomer non-polar interactions, centered around Val-36 (fourth strand, amino domain), and involving, among other residues, Ile-26 (third strand, amino domain) of the

Table 1. Simulation protocols

No. of steps	Method of calculations	Environment	Constraints	Conditions	Dielectrics
20000	minimisation[a]	vacuum	position, all C^{α}	–	linearly distance-dependent
20000	simulated annealing	vacuum	position, all C^{α} improper dihedrals for all chiral centers peptide bonds	–	linearly distance-dependent

No. of steps	Stage	Duration, ps	T_0[b]	TAUTP[c]
0–1000	1. fast heating	1	0–1200 (linear)	0.2
1001–3000	2. hot equilibration	2	1200	0.2
3001–11000	3. slow cooling(a)	8	0	4
11001–13000	4. slow cooling(b)	2	0	1
13001–18500	5. slow cooling(c)	5.5	0	0.5
18501–20000	6. slow cooling(d)	1.5	0	0.05

20000	minimisation	vacuum	position, all C^{α}	–	linearly distance-dependent
20000	minimisation	water	position, all C^{α}	periodic boundary[d,e]	constant
20000	minimisation	water	–	periodic boundary[d,e]	constant
10 runs each 0.1 ps long[f]	molecular dynamics (thermal equilibration)	water	–	periodic boundary[d,e], constant E, p	constant
111 ps; 1 fs step	molecular dynamics	water	SHAKE option enabled	periodic boundary[d,e], constant T, p	constant

[a]After 1000 steps each minimisation was switched from steepest descent to the conjugate gradient mode; [b]In K. This is the temperature of a generic environment thermally coupled with the simulated object by the parameter TAUTP; [c]TAUTP is a temperature relaxation time inversely related to the heat conductivity between the object and the generic environment; [d]Typical box size was of 88 Å × 50 Å × 47 Å, the concentration was about 8.0×10^{-3} mol × dm^{-3}. Approximately 5500–5600 TIP3P water molecules [24] were used, total 18000–18500 atoms; [e]residue based cut-off equal to 8 Å; [f]executed 4 times at temp. 10 K, 100 K, 200 K, 300 K; 1fs step.

same unit and Ile-72 and Cys-79 (third and fourth strands, respectively, carboxyl domain) of the opposite unit. Given the $(NPII/VP)_2$ heterotetramer as an example, a more complete picture, including both qualitative (i.e., which?) and quantitative (i.e., to what extent?) assessment which particular residues contribute to these sets of interactions, can be easily inferred from Fig. 6. Thus, the intra- and intermolecular interactions characterized for $(NPII/VP)_2$ and $(NPI/OT)_2$ reveal that, including both monomers, there are not less than 4 hydrophobic amino-acid residues from either unit to be engaged into the intermonomer interface. In addition, in the NPI/OT complex [16] H-bond contributions from Ser-25 O^{γ} in one NP unit to Glu-81 O^{ε} in the other unit (and *vice versa*, NPI amino acid numbering) are observed. This pair of interactions is precluded in NPII, which has Thr instead of Glu in position 81 (see Fig. 1). Apart from this polar feature unique to NPI, most of the contributions, non-polar in character and involving the

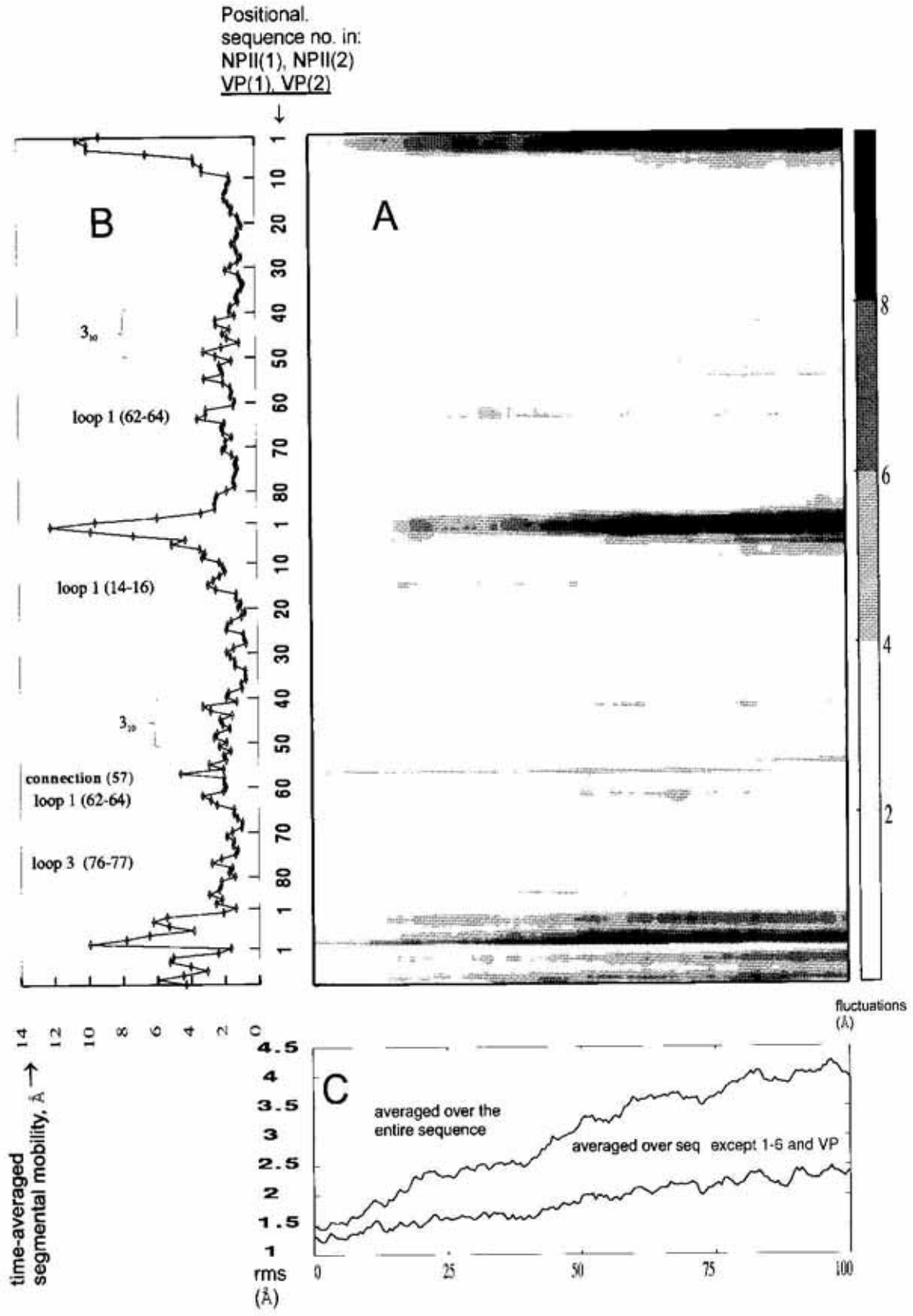
Positional.
sequence no. in:
NPII(1), NPII(2)
VP(1), VP(2)
B
A
C
loop 1 (62-64)
loop 1 (14-16)
connection (57)
loop 1 (62-64)
loop 3 (76-77)
fluctuations
(Å)
time-averaged
segmental mobility, Å
rms
(Å)
averaged over the
entire sequence
averaged over seq except 1-6 and VP

Figure 2.

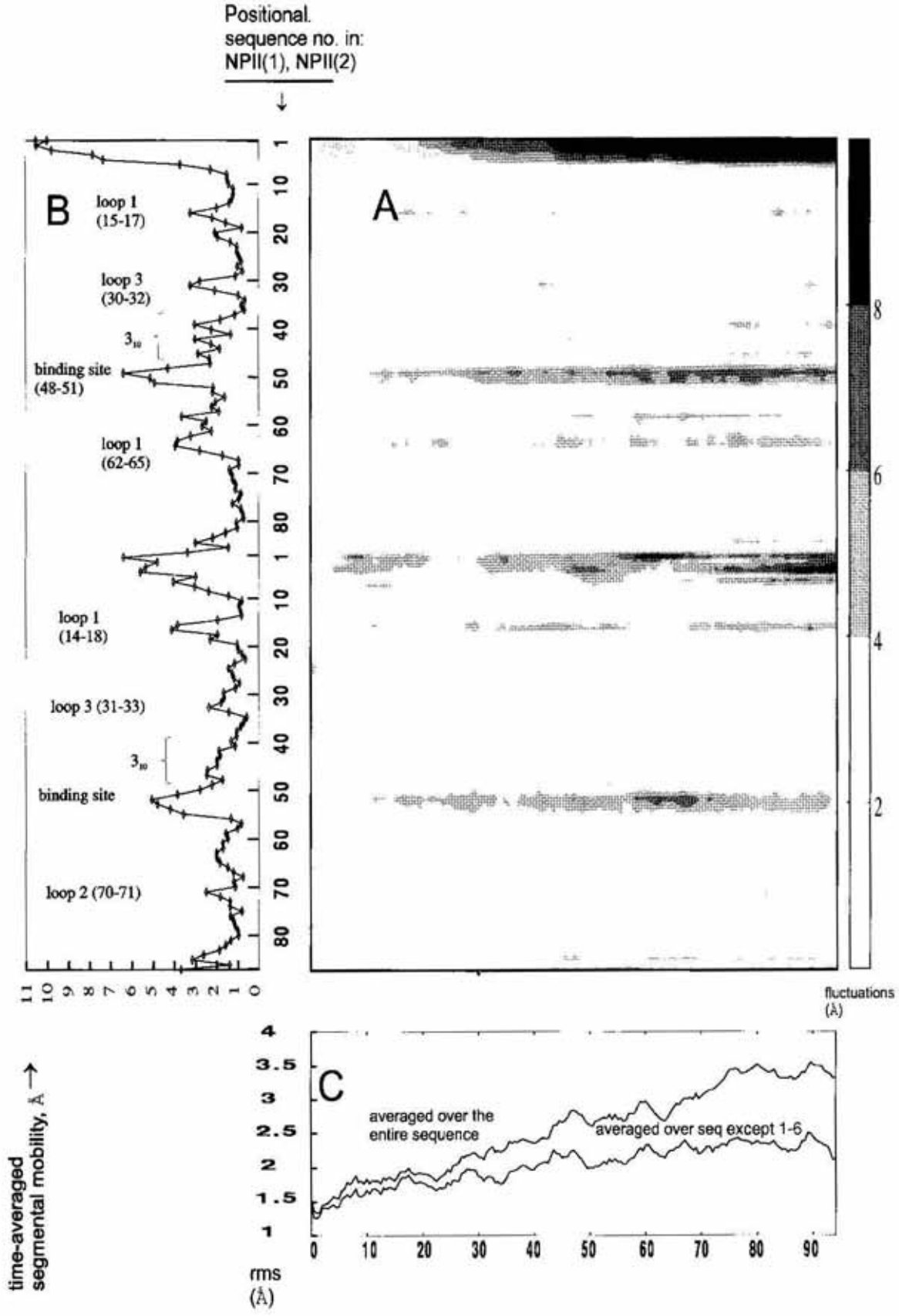
Positional
sequence no. in:
NPII(1), NPII(2)
B
loop 1
(15-17)
loop 3
(30-32)
3₁₀
binding site
(48-51)
loop 1
(62-65)
loop 1
(14-18)
loop 3 (31-33)
3₁₀
binding site
loop 2 (70-71)
A
fluctuations
(Å)
time-averaged
segmental mobility, Å
C
averaged over the
entire sequence
averaged over seq except 1-6
rms
(Å)

Figure 3

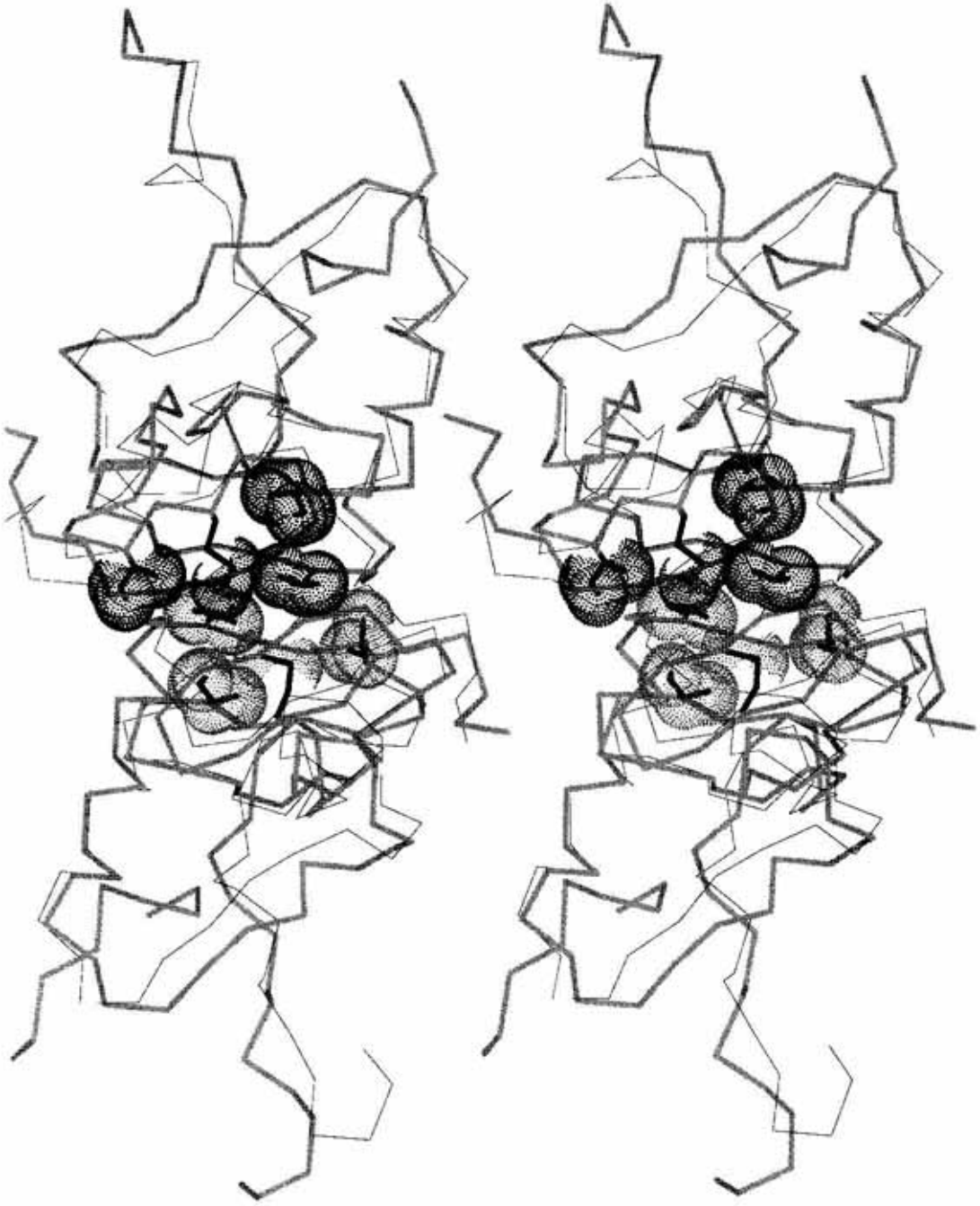

Figure 4

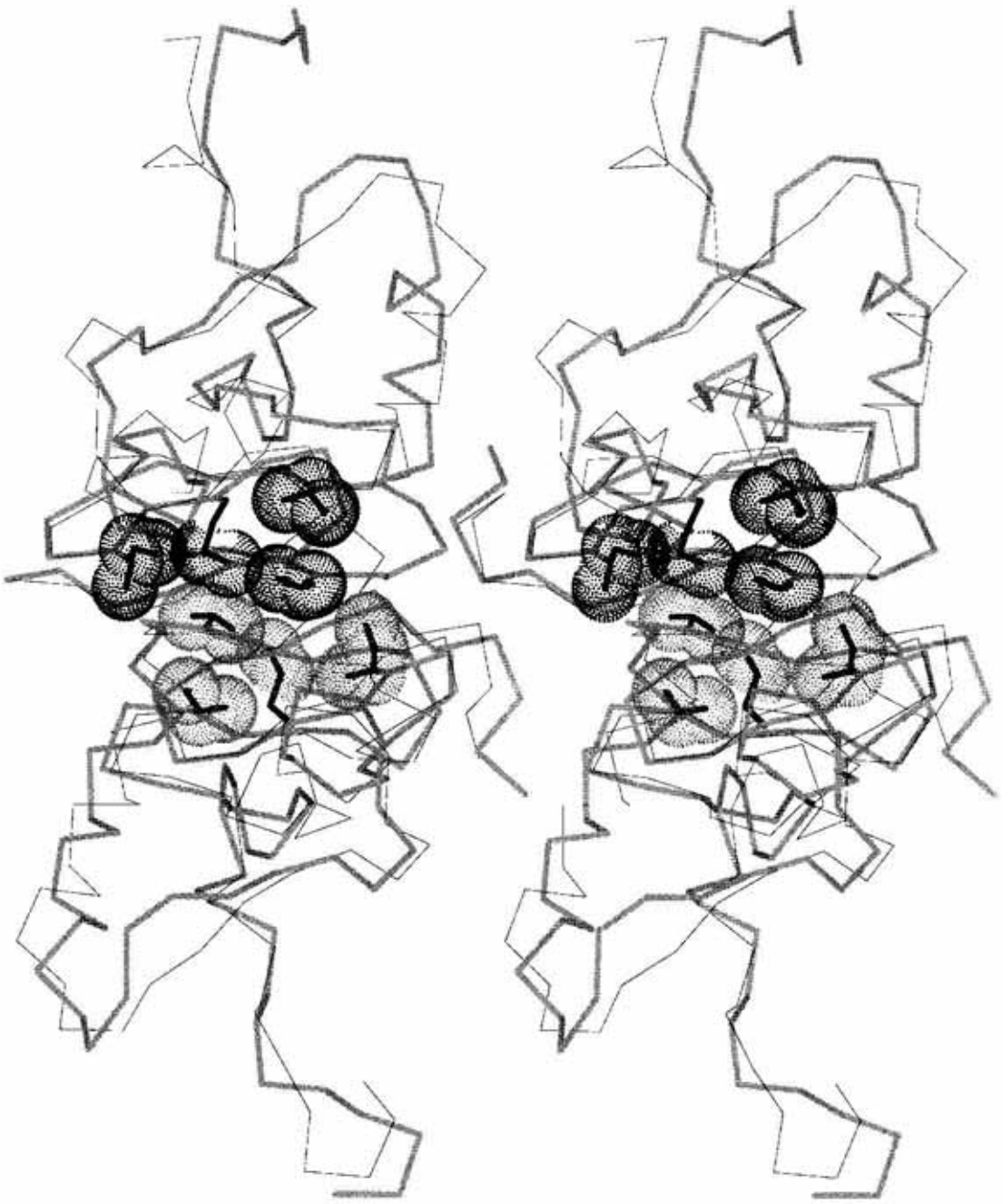

Figure 5

Figure 2. Panel A: The contour plot illustrating the evolution of the geometry in the (NPII/VP)$_2$ heterotetramer over the time range of 100 ps.

Increasing contour shading (see the scale on the far right) corresponds to the increasing fluctuations relative to the starting structure.

Figure 2. Panel B: Time-averaged segmental (NPII/VP)$_2$ mobility.

For easier reference, selected structure features, applying to Panel A as well, are listed on the drawing. The N-terminal residues 1–6, being disordered in any monomer of the template [12], fluctuate most significantly in MD. Some loops are also quite mobile. Substantial fluctuations are seen in the VP C-terminal tails (residues 7–9) and somewhat smaller ones in the exposed parts of the tocin ring (residues 3–5).

Figure 2. Panel C: The build-up of the r.m.s. (root-mean-square) deviation over 100 ps of MD.

After removal of the contributions from the most significant fluctuations at the NPII N-termini and in the VP ligands (compare Panels A and B), the r.m.s. drops dramatically.

Figure 3. The evolution of geometry in the NPII$_2$ homodimer during 104 ps. Given the absence of the VP ligand, other details are the same as in the legend to Fig. 2.

Figure 4. A stereoview of the (NPII/VP)$_2$ heterotetramer structure (thick gray) resulting from the time-averaging of the last 20 ps of MD.

It is overlapping the NPII$_2$ structure taken from Brookhaven PDB (accession code 1BN2) as a reference (thin black). The side chains along with the respective van der Waals zones of Ile-26(1), Val-36(1), Cys-79(2) and Ile-72(2) and their symmetry-related set of Ile-26(2), Val-36(2), Cys-79(1) and Ile-72(1) are indicated, as selection of those residues possibly contributes to the inter-unit allosteric switch. The Figure was generated using RasMol [22].

Figure 5. A stereoview of the NPII$_2$ homodimer structure resulting from the time-averaging over the last 20 ps of MD.

For details see legend to Fig. 4.

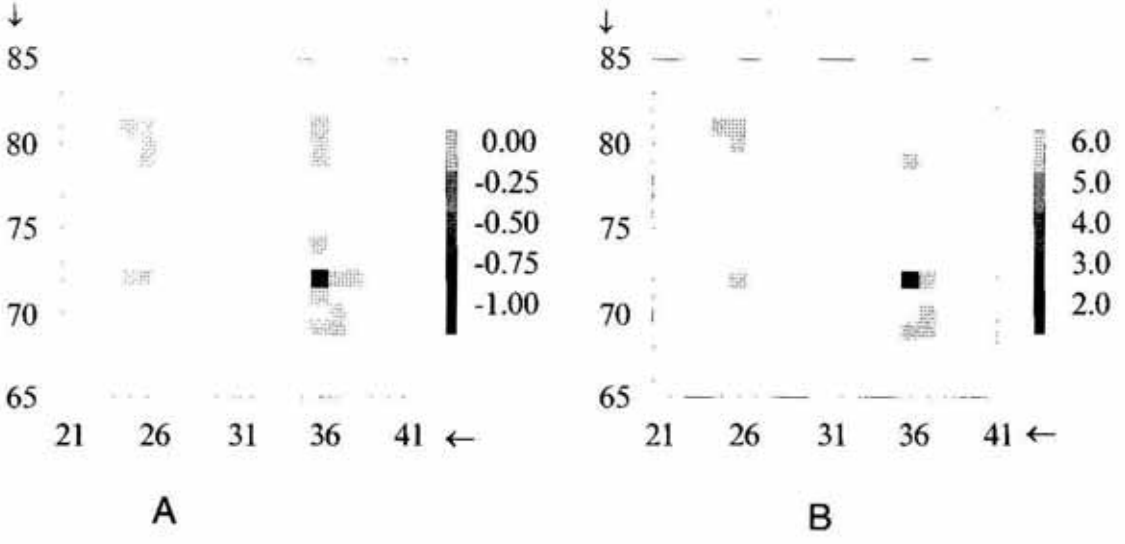

Figure 6. The maps of interactions around and among the residues marked in Fig. 4.

Horizontal axis: Amino-acid sequence comprising Ile-26(1) and Val-36(1) in the amino domain of Unit 1. Vertical axis: Amino acid sequence comprising Ile-72(2) and Cys-79(2) in the carboxyl domain of Unit 2. **Panel A**: the contours represent the inter-residue interaction energy terms with increasing shading for increasing (i.e. more negative) interaction energy, as given by the scale on the right (kcal/mol). **Panel B**: the contours represent the inter-residue minimal distances with increasing shading for decreasing distance, as given by the scale of shading on the right (Å).

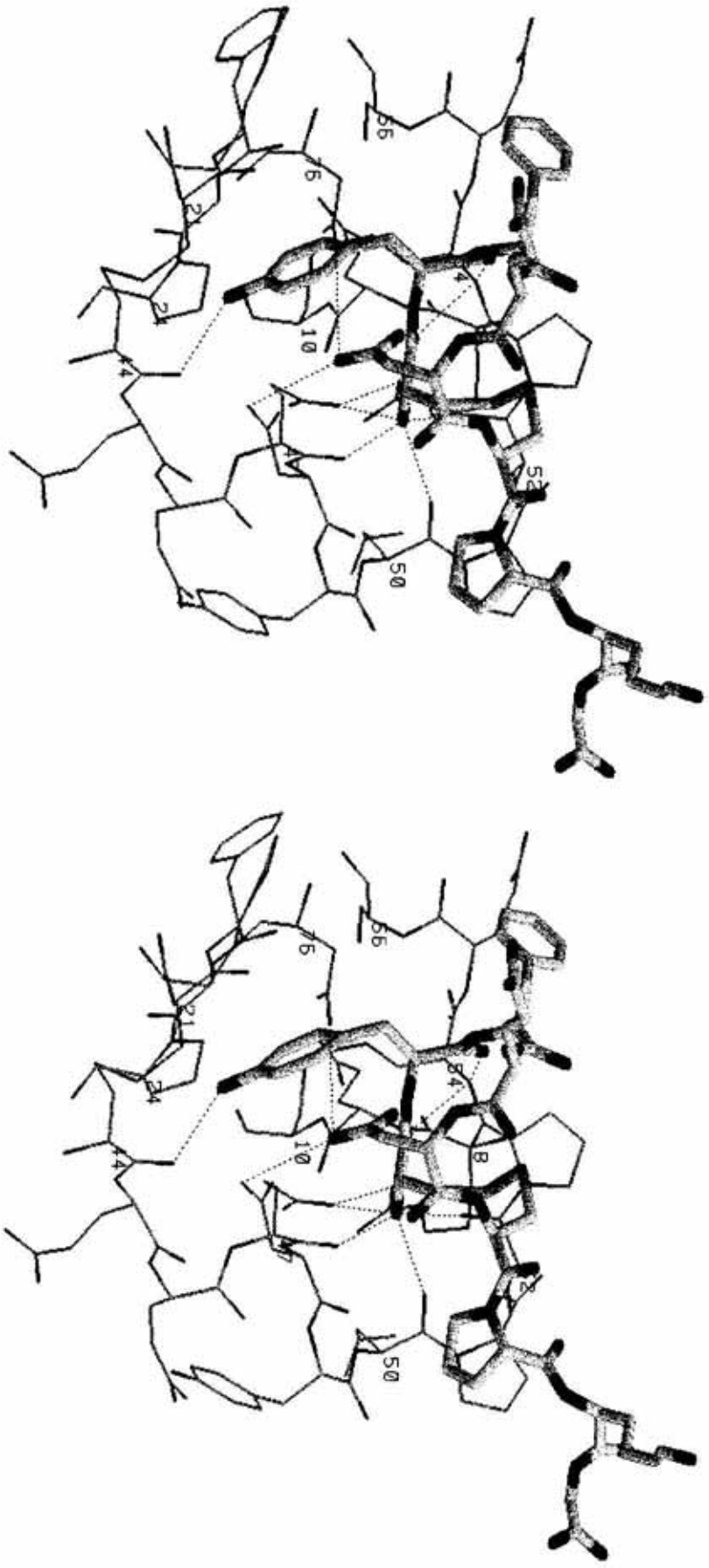

Figure 7

Figure 8

amino domain second loop/third strand link (GPSI, 23–26) and the fourth strand/3_{10} helix base (VGT, 36–38) in the first(second) NPI unit, and the carboxyl domain third (AGICCS, 70–75) and fourth strands (HEDP, 80–83) in the second(first) NP unit, remain similar in both NPI and NPII. The contact distances among side chains of the relevant residues (see Fig. 6B) range between 3–8 Å. These results provide support for a possible ligand-induced interdomain interunit communication and for the role this communication could play in the mutual dependence between the ligand binding and NPI dimerization [16, 17].

From the sequence-distributed time-averaged fluctuations of the $(NPII/VP)_2$ heterotetramer (plotted along the vertical axes in Figs. 2 and 3) it is also seen that the NPII carboxyl domains consistently appear more mobile than their amino counterparts. The same was observed for the $(NPI/OT)_2$ and NPI_2 complexes (not shown).

Figure 7 presents a magnified view of the binding site of unit 2. The binding site in the other monomer (not shown) looks very similar. The Figure is so aligned as to comply as much as possible with Fig. 4 in Ref. [13]. All vital interactions observed both between the N-terminal peptide and NPII [12] and between OT and NPII [13] have been predicted in our NPII/VP complex. Moreover, the arrangements and orientations of the side chains of the amino-acid residues directly contributing to the NPII/VP interface are very similar to those reported in the solid state structures. Detailed comparison is given in Ref. [16]. Figure 8 gives an idea of how far the VP tocin rings from both units 1 and 2 [17] overlap each other and that of OT in unit 2 [16]. The latter was proven [16] to overlap well the OT conformation in the NP/OT solid state structure [13]. With the r.m.s. deviation values for the C^{α} atoms equal to 0.9 Å, 1.11 Å and 0.57 Å, for the OT2/VP1, OT2/VP2 and VP1/VP2 pairs, respectively, and virtually perfect overlap within the C1..Y2..C6 pharmacophores, it is seen that the OT part directly interacting with NPI [16] and the VP part directly interacting with NPII exhibit to a very high extent common modes of interactions with the respective NPs and these modes are in complete agreement with those observed in the solid state structures [12, 13]. The common modes of interaction in the NPI/OT and NPII/VP complexes explain the ability of both hormones and both proteins to produce cross-complexes *in vitro* [4, 5]. Simultaneously, a relative flexibility of the remaining parts of the hormones is clearly seen; see also Fig. 2. To sum up, this minireview indicates that, given a carefully chosen modeling protocol (see Table 1), a low-resolution structure like a mere C^{α}-trace may be refined to an all-atom representation that not only reproduces all real molecular interactions with high fidelity but also may serve as a tool for predicting new, not so far reported, molecular properties.

REFERENCES

1. Land, H., Grez, M., Ruppert, S., Schmale, H., Rehbein, M., Richter, D. & Schutz, G. (1983) Deduced amino acid sequence from the bovine oxytocin-neurophysin I precursor cDNA. *Nature* **302**, 342–344.

Figure 7. A stereoview of VP in its binding site.

This is an enlarged fragment of the structure drawn in Fig. 4 so aligned as to comply as much as possible with the view in Fig. 4 of Ref. [13]. The Figure was generated using RasMol [22].

Figure 8. A stereoview of three overlapping hormone structures in their binding sites: OT in unit 2 [16] (thin, black), VP unit 1 (thick, gray) and VP unit 2 (thick, black) [17].

It is seen that the peptide bonds between residues 2 and 3 in VP and OT are in approximately opposite orientations. The Figure was generated using MolScript [23].

2. Land, H., Schutz, G., Schmale, H. & Richter, D. (1982) Nucleotide sequence of cloned cDNA encoding bovine arginine vasopressin-neurophysin II precursor. *Nature* **295**, 299–303.

3. Dreifuss, J.J. (1975) A review of neurosecretory granules: Their contents and mechanism of release. *Ann. N. Y. Acad. Sci.* **248**, 184–201.

4. Breslow, E. & Burman, S. (1990) Molecular, thermodynamic, and biological aspects of recognition and function in neurophysin-hormone systems: A model system for the analysis of protein-peptide interactions. *Adv. Enzymol.* **63**, 1–67.

5. Breslow, E. & Walter, R. (1972) Binding properties of bovine neurophysin I and II: An equilibrium dialysis study. *Molecular Pharmacology* **8**, 5–81.

6. Breslow, E. (1978) Chemistry and biology of the neurophysins. *Annu. Rev. Biochem.* **48**, 251–274.

7. Menendez-Botet, C. & Breslow, E. (1975) Chemical and physical properties of the disulphides of bovine neurophysin-II. *Biochemistry* **14**, 3825–3835.

8. Chaiken, I.M., Randolph, R.E. & Taylor, H.C. (1975) Conformational effects associated with the interaction of polypeptide ligands with neurophysins. *Ann. N.Y. Acad. Sci.* **248**, 442–450.

9. Kanmera, T. & Chaiken, I.M. (1985) Molecular properties of the oxytocin/bovine neurophysin I biosynthetic precursor. Studies using a semisynthetic precursor. *J. Biol. Chem.* **260**, 8474–8482.

10. Ando, S., McPhie, P. & Chaiken, I.M. (1987) Sequence redesign and the assembly mechanism of the oxytocin/bovine neurophysin I biosynthetic precursor. *J. Biol.Chem.* **262**, 12962–12969.

11. Huang, H.B. & Breslow, E. (1992) Identification of the unstable neurophysin disulphide and localization to the hormone-binding site. Relationship to folding-unfolding pathways. *J. Biol. Chem.* **267**, 6750–6756.

12. Chen, L., Rose, J.P., Breslow, E., Yang, D., Chang, W.-E., Furey, W.F., Jr., Sax, M. & Wang, B.-C. (1991) Crystal structure of a bovine neurophysin II dipeptide complex at 2.8 Å determined from the single-wavelength anomalous scattering signal of an incorporated iodine atom. *Proc. Natl. Acad. Sci. U.S.A.* **88**, 4240–4244.

13. Rose, J.P., Wu, Ch.-K., Hsiao, Ch.-D., Breslow, E. & Wang, B.-C. (1996) Crystal structure of the neurophysin-oxytocin complex. *Nature Struct. Biol.* **3**, 163–169.

14. Kaźmierkiewicz, R., Czaplewski, C., Lammek, B. Ciarkowski, J. & Lesyng, B. (1995) Study of the interactions between neurophysin II and dipeptide ligand by means of molecular dynamics. *J. Mol. Model.* **1**, 135–141.

15. Bernstein, F.C., Koetzle, T.F., Williams, G.J., Meyer, E.E.J., Brice, M.D., Rodgers, J.R., Kennard, O., Shimanouchi, T. & Tsanumi, M. (1977) The protein data bank: A computer-based archive file for macromolecular structures. *J. Mol. Biol.* **112**, 535–542.

16. Kaźmierkiewicz, R., Czaplewski, C., Lammek, B. & Ciarkowski, J. (1997) Molecular modeling of the neurophysin I/oxytocin complex. *J. Comp. Aided Molec. Design* **11**, 9–20.

17. Kaźmierkiewicz, R., Czaplewski, C., Lammek, B. & Ciarkowski, J. (1997) Molecular modeling of the neurophysin II/vasopressin complex. *Quant. Struct.-Act. Relat.* **16**, 193–200.

8. SYBYL, v. 6.1 (1994) Tripos Inc., St. Louis, MO, U.S.A.

19. Lippens, G., Hallenga, K., Van Belle, D., Wodak, S.J., Nirmala, N.R., Hill, P., Russell, K.C., Smith, D.D. & Hruby, V. (1993) Transfer nuclear Overhauser effect study of the conformation of oxytocin bound to bovine neurophysin I. *J. Am. Chem. Soc.* **32**, 9423–9434.

20. Breslow, E., Sardana, V., Deeb, R., Barbar, E. & Peyton, D.H. (1995) NMR behavior of the aromatic protons of bovine neurophysin-I and its peptide complexes: Implications for solution structure and for function. *Biochemistry* **34**, 2137–2147.

21. Pearlman, D.A, Case, D.A., Caldwell, J.W., Ross, W.S., Cheatham III, T.E., Ferguson, D.M., Seibel, G.L., Singh, U.C., Weiner, P.K.

& Kollman, P.A. (1995) AMBER 4.1. University of California, San Francisco, CA, U.S.A.

22. Sayle, R. (1996) RasMol v. 2.6. Molecular Visualisation Program, Glaxo Wellcome Research and Development, Stevenage, Hertfordshire, U.K.

23. Kraulis, P. (1991) MOLSCRIPT: A program to produce both detailed and schematic plots of protein structures. *J. Appl. Crystallogr.* **24**, 946–950.